



Interaction Between Coronal Mass Ejection "CMEs" and Jupiter Magnetosphere by Numerical Simulation Using MHD Models

Wafaa H. Zaki

University of Kirkuk/College of Science/Department of Physics

hassanf99@yahoo.com

ABSTRACT

The present study deals with the interaction between the magnetic field of Jupiter and ones of the Coronal Mass Ejections (CMEs) for three years (2011-2013) which includes the peak of Solar cycle 24. These interactions were studied through numerical simulation using Magneto hydrodynamic models (MHD) and solved numerically by Leapfrog method with the aid of MATLAB program. The data related to CMEs were derived from LASCO/SOHO, and were verified whether there are events or not by checking them from ERNE detectors (LASCO and ERNE are scientific systems on board SOHO). While the data which concern with Jupiter were taken from VOYAGER 1. The simulation were achieved in two stages; firstly, the beginning simulation of the launched CMEs from the surface of the Sun until they reach behind the boundary of the magnetosphere of Jupiter through interplanetary using the ideal MHD model (conservative model), and secondly is being the simulation of the interaction between the magnetic field of the CMEs and ones of Jupiter. It is verified using Semi-relativistic MHD model. Accordingly, it was found that Leapfrog numerical analysis is the optimal and best method. In addition, the outgoing CMEs to Jupiter embraces impulsive type and associated with Flares. Furthermore, it has been noted from the numerical simulation that intensity of the final magnetic field after the interaction of CMEs magnetic field with Jupiter magnetic field is going to increase giving rise to positive correlation with the speed of the adopted CMEs. On the other hand, the fast MHD shock wave with convex surface was created, because the speed of the adopted CMEs were greater than Alfven speed.

Keywords: Solar activity, Solar cycle 24, SOHO-LASCO-ERNE: data base, MHD models, Numerical simulation, Jupiter.



تفاعل المجال المغناطيسي للمقذوفات الأكليلية الشمسية مع المجال المغناطيسي لكوكب المشتري من خلال المحاكاة العددية باستخدام نماذج MHD

وفاء حسن علي زكي

جامعة كركوك/ كلية العلوم/ قسم الفيزياء

hassanf99@yahoo.com

الملخص

في هذه الدراسة تم التحقق من التفاعل بين المجال المغناطيسي للمقذوفات الأكليلية الشمسية CME مع المجال المغناطيسي لكوكب المشتري للسنيين ٢٠١١، ٢٠١٢ و ٢٠١٣ والتي هي ضمن قمة الدورة الشمسية ٢٤، وذلك من خلال المحاكاة العددية باستخدام النماذج الهيدروديناميكية المغناطيسية MHD وحلها بطريقة التحليل العددي لليفروك Leapfrog وبواسطة البرنامج ماتلاب. تم أخذ البيانات المتعلقة بالمقذوفات الأكليلية من المنظومة لاسكو LASCO والتحقق منها فيما إذا كانت إحداث شمسية أم لا وذلك من خلال كواشف إيرنا ERNE (لاسكو وايرنا هي انظمه محمولة على المختبر الفضائي سوهو)، أما البيانات المتعلقة بكوكب المشتري فقد تم أخذها من فويجر ١. أنجزت المحاكاة العددية في هذه الدراسة بمرحلتين، المرحلة الأولى، هي محاكاة المقذوفات الأكليلية الشمسية منذ انطلاقها من سطح الشمس مروراً بفضاء ما بين الكواكب وحتى وصولها إلى حافة المجال المغناطيسي للمشتري وباستخدام النموذج MHD المثالي (المحافظ)، أما المرحلة الثانية هي عند تفاعل المجالات المغناطيسية لكل من المشتري والمقذوفات الأكليلية وإعادة اتصالهم وهنا تم استخدام النموذج MHD الشبه النسبي (غير المحافظ). لقد تبين من هذه الدراسة إن طريقة التحليل العددي لليفروك هي الأنسب والأمثل في حل معادلات النماذج الهيدروديناميكية المغناطيسية. وقد وجد من هذه الدراسة إن المقذوفات الأكليلية الشمسية المتجه نحو كوكب المشتري هي من النوع الدفعي وعادة تكون مصاحبة للتأججات الشمسية. و لوحظ أيضاً من خلال المحاكاة ان شدة المجال المغناطيسي بعد التفاعل يزداد كلما زادت سرعة المقذوفات الأكليلية الشمسية المعتمدة في هذه الدراسة، وعندما تصل هذه السرعة إلى أكبر من سرعة ألفن ستتكون موجة الصدمة السريعة وتكون محدبة الشكل.

الكلمات الدالة: النشاط الشمسي، المقذوفات الأكليلية الشمسية، الدورة الشمسية ٢٤، قاعدة بيانات: سوهو - لاسكو - إيرنا، النماذج الهيدروديناميكية المغناطيسية MHD، المحاكاة العددية، كوكب المشتري.



1. INTRODUCTION

As it is known that the Solar system consists of the Sun and the planets, the largest of these planets is Jupiter which features huge and complex magnetic field. Also the Sun has a large and complex magnetic field and goes through what it call a Solar activity cycle, where every 11 year it will go from a very low period of solar activity, meaning a Sun spot and solar wind to another period of law activity and in between it goes through what it is call solar maximum. At solar maximum, sun has a very complicated magnetic field structure, and therefore it creates a lot more sun spot and solar wind like" flare, Solar Energetic Particles(SEPs) and Coronal Mass Ejections(CMEs)" [1][2]. Solar activity have played a large role in the formation and evolution of the" Solar system" particularly affecting the magnetic fields of a planet that has a well-developed magnetic field (such as Earth, Jupiter and Saturn) [3]. As mentioned earlier on the components of the Solar Wind, the Flares are electromagnetic spectrum and SEP are solar particles of high energies made up of Protons and Electrons and sometimes associated by Neutrino particles as well as the Coronal Mass Ejections (CMEs). Coronal Mass Ejections (CMEs) are unexpected releases of ionized gas from the Sun surface into interplanetary space. These explosions are triggered by a very complicated mechanism, but it is thought to involve slow storage of magnetic energy that is quickly released by means of magnetic reconnection. In the solar case, following the eruption, CMEs are accelerated in the corona, some to high terminal speeds of up to 3000 km s⁻¹, where their magnetic integrity "commonly referred to as the magnetic cloud" is maintained as they are propagating to large interplanetary distances up to a point beyond 5.2 A.U [4]. It is known that Jupiter away from Sun by 5.2 A.U, thus, it is within the incidence of the CMEs, on this basis there will be an interaction between the magnetic field of Jupiter and the magnetic field of the CMEs. Simulation is the most appropriate way to verify this study and will be in two steps. So the main goal of this study, first, simulate the CMEs itself from the beginning of their growth and spread in the interplanetary by using the ideal magneto hydro dynamic model MHD until are reaches Jupiter.



Second, simulate the interaction between the magnetic field of Jupiter and the CMEs using semi-relativistic MHD model. As well as the huge magnetic field of Jupiter does protect Earth from comets and also pull a giant mass of the coronal mass ejections (CMEs) that may be impact the Earth.

2. MAGNETO HYDRODYNAMIC MODELS MHDs

2.1. IDEAL MHD MODEL

In ideal MHD model, Lenz's law dictates that the fluid is in a sense-tied to the magnetic field lines and a small rope-like volume of fluid surrounding a field line will continue to lie along a magnetic field line, even as it is twisted and distorted by fluid flows in the system. The connection between magnetic field lines and fluid in ideal MHD fixes the topology of the magnetic field in the fluid—for example, if a set of magnetic field lines are tied into a knot, and then they will remain so as long as the fluid/plasma has negligible resistivity. This difficulty in reconnecting magnetic field lines makes it possible to store energy by moving the fluid or the source of the magnetic field. The energy can then become available if the conditions for ideal MHD break down, allowing magnetic reconnection that releases the stored energy from the magnetic field [5]. As is well known the Coronal Mass Ejections (CMEs) consists of coronal plasma confined within a conservative magnetic field, so the ideal MHD model is very appropriate model to simulate the CMEs cross the interplanetary until it reaches the edge of the surface layer of the magnetosphere of Jupiter[6]. The plasma of the CMEs is described by a set of fluid equations in the conservative state of mass[7]. And this plasma have infinite electrical conductivity and the magnetic field assumed to be "Frozen" into plasma[8]. In this investigation the equations of the ideal MHD model that describe the dynamic of plasma under the influence of a magnetic field will be as follows[9]:

$$\frac{\partial \rho}{\partial t} + \nabla \cdot (\rho v) = 0 \quad (1)$$



$$\frac{\partial v}{\partial t} - v \nabla v + \frac{1}{2} v \rho + \frac{B}{4\pi\rho} \nabla B = 0 \quad (2)$$

$$\frac{\partial B}{\partial t} = [\nabla x(vxB)] \quad (3)$$

$$\frac{\partial \rho}{\partial t} + v \frac{\partial \rho}{\partial x} + \gamma \rho \frac{\partial v}{\partial x} \quad (4)$$

$$e = \frac{\rho v^2}{2} + \frac{\rho}{\gamma - 1} + \frac{B^2}{8\pi} \quad (5)$$

Where (ρ) is the mass density of plasma, (n) is a number of particles, (p) is a pressure, (v) is the velocity, (e) is the total energy density and (B) is a magnetic field, where (γ) is a polytropic index of plasma and it is equal to 5/3.

2.2. SEMI-RELATIVISTIC MHD MODEL

To achieve the study of the interaction between the CMEs and the magnetosphere of Jupiter as it is pointed before " by numerical simulation" , so the Semi-relativistic MHD model is the best suited for this study. This model used when classical Alfvén speed (V_A) larger than the speed of light (C) and that is exactly for the case of interaction with Jupiter's magnetosphere which is very strong field due to the strong planetary magnetic field and have moderate Alfvén speed (V_A), and this speed is not bounded by the speed of light near strongly magnetized planets " Jupiter"[10]. For this study, the primitive –variable equation set of the Semi- relativistic MHD model with anisotropic ion pressure and isotropic electron pressure[11]. This equations starts with the non-conservative form of the nonrelativistic MHD equations with electric force in the momentum equation and displacement current in Ampère's law[12]:

$$\frac{\partial \rho}{\partial t} + (v \cdot \nabla) \rho + (v \cdot \nabla) = 0 \quad (6)$$

$$\rho \frac{\partial v}{\partial t} + \rho (v \cdot \nabla) v + \nabla p - j \times B - qE = 0 \quad (7)$$



$$\frac{\partial B}{\partial t} + \nabla \times [-(v \times B)] = 0 \quad (8)$$

$$\frac{\partial \rho_e}{\partial t} + (v \cdot \nabla) \rho_e + \frac{5}{3} \rho_e (\nabla \cdot v) = 0 \quad (9)$$

4. DATA HUNDLING

In this approaches high speed CMEs of type halo will detected as three important events during the Solar Cycle 24, and these CMEs have been detected and selected from SOHO/ ERNE[13]. The adopted events have a clear background with intensities greater than " $10^{-3} \text{ cm}^{-2} \text{ sr}^{-1} \text{ s}^{-1} \text{ Mev}^{-1}$ " for each "1-116 Mev" , and that are:

1. For the year 2011 (1-15.08)
2. For the year 2012 (26-27.05)
3. For the year 2013 (10-15.04)

All these data are available at "ERNE DATA FINDER"[13]. The calculations are illustrated in figures (1,2 and 3) shows the SEPs onset at the associated phenomena for these three selected events.

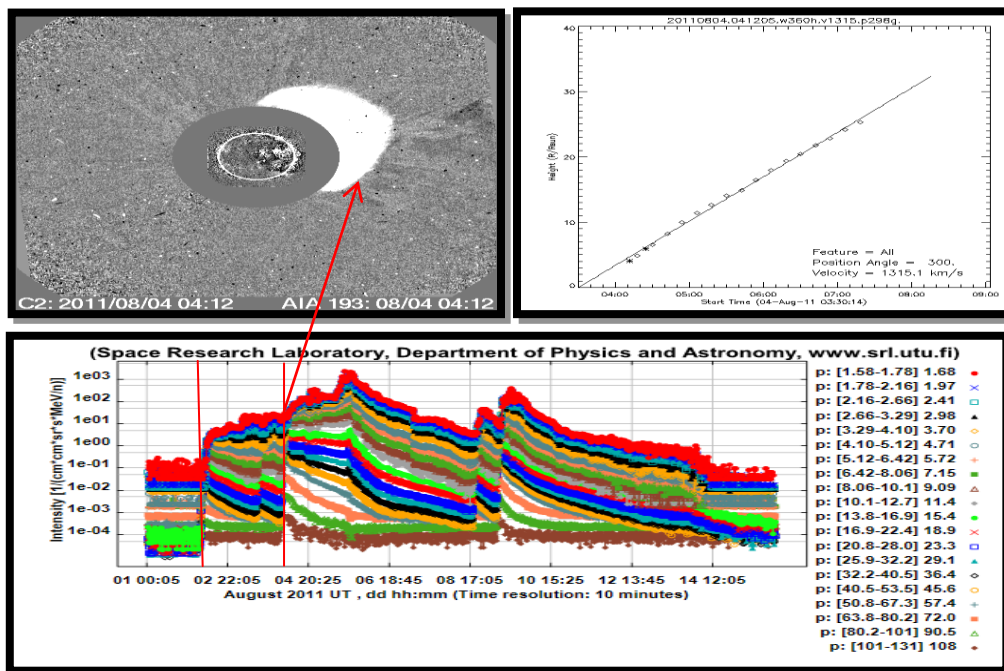


Figure (1): Shows the analysis of the events (1-15) August 2011: The down image illustrates the intensity-time profile from ERNE/SOHO with resolution time of 10 minute, the red lines are represents numbers of associated CMEs. The upper left image indicate the first appearance time of CMEs . The third right image is the linear speed fitting.

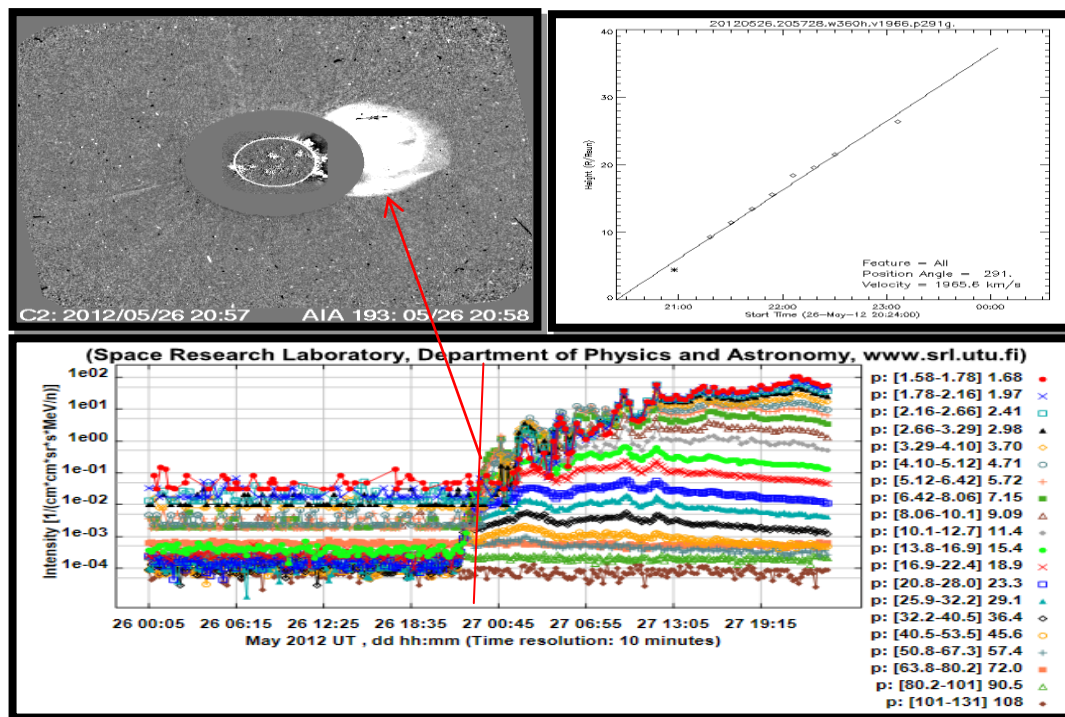
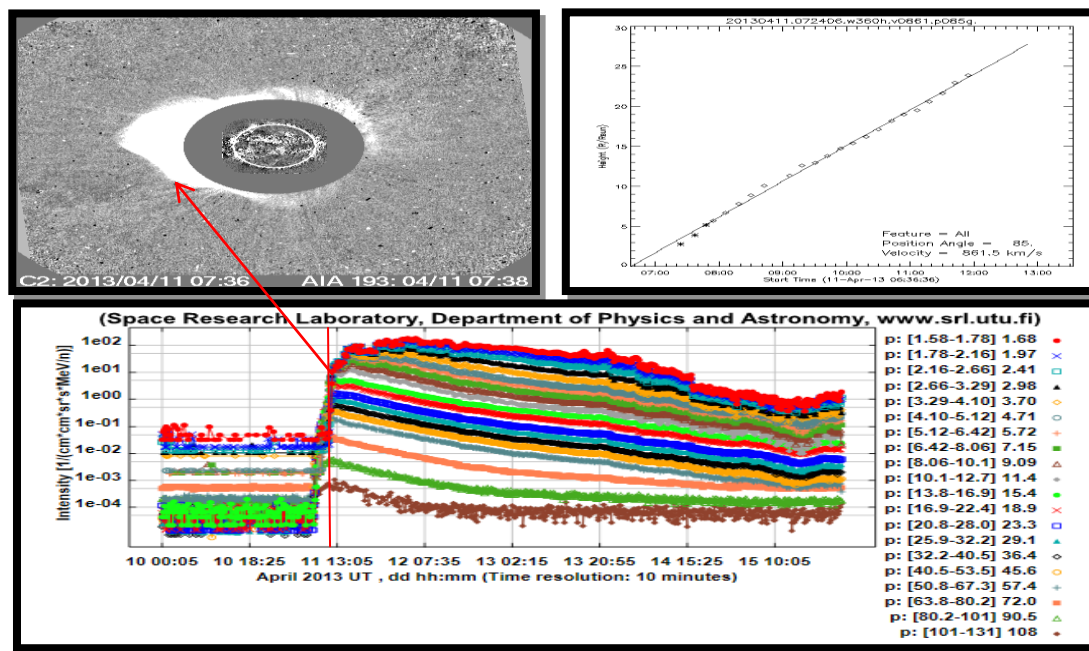


Figure (2): Shows the analysis of the events (26-27) May 2012: The down image illustrates the intensity-time profile from ERNE/SOHO with resolution time of 10 minute, the red lines are represents numbers of associated CMEs. The upper left image indicate the first appearance time of CMEs . The third right image is the linear speed fitting.



Figure(3): Shows the analysis of the events (10-15) April 2013: The down image illustrates the intensity-time profile from ERNE/SOHO with resolution time of 10 minute, the red lines are represents numbers of associated CMEs. The upper left image indicate the first appearance time of CMEs . The third right image is the linear speed fitting.

All data related to the CMEs will be analyzed and calculated through the associated SEPs three events and all features must be calculated in order to employing them in the present simulation.

5. METHODS OF CALCULATING CMEs



ERNE was designed to measure the upper range of the Solar Energetic Particles (SEPs) and it is capable to analogy the differential energy spectra of Protons and Helium in the range (1.3-140 MeV)[14]. The classes of events produce inconsistent range of Protons energies and intensities[15]. According to this difference between the Protons, Electrons and heavy ions by means of velocity and weight, the intensity-time profile is more suitable to protons than other particles. The Onset time and the injection time will be calculated from the intensity-time profile for the adopted three events in this study[16].

$$T_{inj} = (t_0 - t_f) + 8.3min \quad (10)$$

T_{inj} = The time when particles release from the source.

t_0 = Onset time observed by the ERNE

t_f = Flight time of particles during flight from source to ERNE.

The flight time can be realized using beta equation,

$$\beta = v/c \quad (11)$$

Where v = the speed of particles = s/t_f , c = the speed of light, (8.3 min) have been added to represent the time of light to reach the Earth from the Sun. Then the flight time (t_f) founded by:

$$t_f = s/\beta c \quad (12)$$

Where s is the fixed path length for the particles which equal the distance between the Sun and the detector (=1.2 AU), and β equal

$$\beta = \left[1 - (p/(E + p))^2 \right]^{1/2} \quad (13)$$

P is the energy of proton= (938 MeV), E is the proton kinetic energy[17]. All these listed in table (1).



No.	DD.MM.YY				
1	(1-15).08.2011	29.1	04:55	4:22	4.08
2	(26-27).05.2012	15.4	21:05	20:18	4.42
3	(10-15).04.2013	23.3	07:55	07:18	2.79

Table(1): Represents the Energy, Onset time, Injection time and the Height of the adopted CMEs

The mass, energy and the density was calculated from the Coronagraph on board SOHO [18]. Where E is the kinetic energy of the CME, m is the mass of the CME and v is the speed of the CME. This features are listed in table(2) .

Table(2): This table illustrated the linear speed, mass and the kinetic energy of the adopted CMEs

No.	First Appearance Date Time[UT]		Linear Speed [Km/s]	Mass [Kg]	Kinetic Energy [Joule]
1	2011/08/09	8:12:06	1610	1.6×10^{13}	2.1×10^{25}
2	2012/05/26	20:57:28	1966	4.9×10^{12}	9.4×10^{24}
3	2013/04/11	07:24:06	861	1.3×10^{13}	4.8×10^{24}

6. IMPLEMENTATION OF JUPITER

Jupiter is a gas giant planet of diameter 11 times that of Earth and its mass 318 times that of Earth, and stay out of the Sun by 5.2 A.U[19]. And it have a huge magnetic field "largest magnetosphere planet" in Solar system, so the Solar wind velocity drops to subsonic speed at the boundary of Jupiter magnetosphere and this speed called The " Bow Shock", which is varying between $55R_j$ - $125R_j$ " R_j is Jupiter radius"[20]. By using the observation of Voyager 1 it can develop probabilistic models of the " Bow Shock" and magnetopause. The method is based on a



combination of the huge data base with a results from MHD simulation of the adopted CMEs dynamic pressures on the "Bow Shock".

Using the model of plasma for the CMEs and field configuration near Jupiter, at time $t=0$ for the simulation box, Where Alfven velocity is very large near Jupiter and placed inner boundary of the simulation at $15R_j$ in order to keep the time step from getting too small. The simulation parameters are fixed at the inner boundary. The azimuthally velocity is set to co-rotate, pressure and density are set from voyager1 flyby Jupiter. And the equatorial field of Jupiter is about 4.3G.

7. APPLICATION OF NUMERICAL SIMULATION

Numerical simulation of this investigation will study the response of the magnetic field of a close planet to the CMEs events using the adopted MHD models as it mentioned before " simulation includes CMEs and the planet Jupiter", which were described by boundary and initial values for temperature, density, pressure, velocity and magnetic field. The numerical model application in this simulation was based on Leapfrog method which is widely used to solve numerical problems, with initial – boundary values and this method is 2nd order accurate in space and time i.e., the accuracy $[(\Delta t)^2, (\Delta x)^2]$ [12].

Two principle steps of Leapfrog method explicit:

1. Using centered scheme on time and space derivative such as,

$$\frac{\partial \rho}{\partial t} = \frac{\rho_i^{n+1} - \rho_i^{n-1}}{\partial t}, \quad \frac{\partial \rho}{\partial x} = \frac{\rho_{i+1}^n - \rho_{i-1}^n}{2\Delta x} \quad (14)$$



2. Using the condition of stability for derivative of space. For the current n^{th} time and state i^{th} space state that are achieved by substituting the average of the variable state for the given degree of freedom, and from equation (1) and equation (14) will produce this equation:

$$\rho_i^{n+1} = \frac{\rho_{i+1}^n + \rho_{i-1}^n}{2} - 2\Delta t \left(v_i^n \left(\frac{\rho_{i+1}^n + \rho_{i-1}^n}{2\Delta x} \right) - \rho_i^n \left(\frac{v_{i+1}^n + v_{i-1}^n}{2\Delta x} \right) + \rho_i^n \right) \quad (15)$$

By using equation (15) the $(n+1)^{\text{th}}$ variable would be in the left side of this equation and n^{th} variable in the right side of the equation. This ensures to calculate the $(n+1)^{\text{th}}$ state of time from the state that came before. Also by applying Leapfrog on the equations (2,3, 4) will produce the following equations respectively:

$$v_i^{n+1} = \frac{v_{i+1}^{n-1} - v_{i-1}^{n-1}}{2} - 2\Delta t \left(v_i^n \left(\frac{v_{i+1}^n - v_{i-1}^n}{2\Delta x} \right) - \frac{1}{\rho_i^n} * \left(\frac{\rho_{i+1}^n - \rho_{i-1}^n}{2\Delta x} \right) - \frac{B_i^n}{4\pi\rho_i^n} * \left(\frac{B_{i+1}^n - B_{i-1}^n}{2\Delta x} \right) \right) \quad (16)$$

$$B_i^{n+1} = \left(\frac{B_{i+1}^n - B_{i-1}^n}{2} \right) + 2\Delta t \left(v_i^n \left(\frac{B_{i+1}^n - B_{i-1}^n}{2\Delta x} \right) + B_i^n \left(\frac{v_{i+1}^n - v_{i-1}^n}{2\Delta x} \right) \right) \quad (17)$$

$$p_i^{n+1} = \left(\frac{p_{i+1}^n - p_{i-1}^n}{2} \right) - v_i^n \Delta t \left(\frac{\rho_{i+1}^n - \rho_{i-1}^n}{2\Delta x} \right) - \gamma \rho_i^n \Delta t \left(\frac{v_{i+1}^n - v_{i-1}^n}{2\Delta x} \right) \quad (18)$$

Since the equations (16), (17) and (18) are the simulation equations in term of each the velocity, magnetic field and pressure respectively.

It will make use of the obtained results for the adopted events as a data of boundary and initial condition for this simulation. The CMEs moves through the inner corona and propagates outward into interplanetary and disabled the heliospheric currents sheets as it moves. At 16-18 hour into the simulation the pressure enhancement will disappear, so the connection between the CMEs field lines and the solar surface will disappear. Boundary and initial conditions for this investigation are very important to solve the simulation, and they were applied at the first step of the program and requires to setting up various matrices during the simulation. The boundary conditions must always applied during each loop and they do not affect the results related to the

initiation and propagation of CMEs. Tables (3) illustrate the boundary and initial conditions for the CME1 event.

Table(3): Initial and boundary conditions for the CME1

Quantity	Initial value	Boundary value
Mass density, (P)[Kg.m ⁻³]	10 ⁻¹²	0.01
Particle velocity(v _x ,v _y ,v _z)[Km. S ⁻¹]	0	2× 10 ⁻³
Magnetic field, [B _x ,B _y ,B _z][nT]	30× 10 ⁻⁴	5× 10 ⁻⁴
Pressure, (P)[nPa]	10 ⁻⁸	10 ⁻⁹

The mass density was calculated from equation (1) and its value increase with the growth of the CME. And from figure(4) has found that the peak was $\approx 1.5 \times 10^{33}$ at Z= 5R_⊙, and at Z= 30R_⊙ the peak become $\approx 2.3 \times 10^{34}$ where Z represents the distance from the radius of Sun.

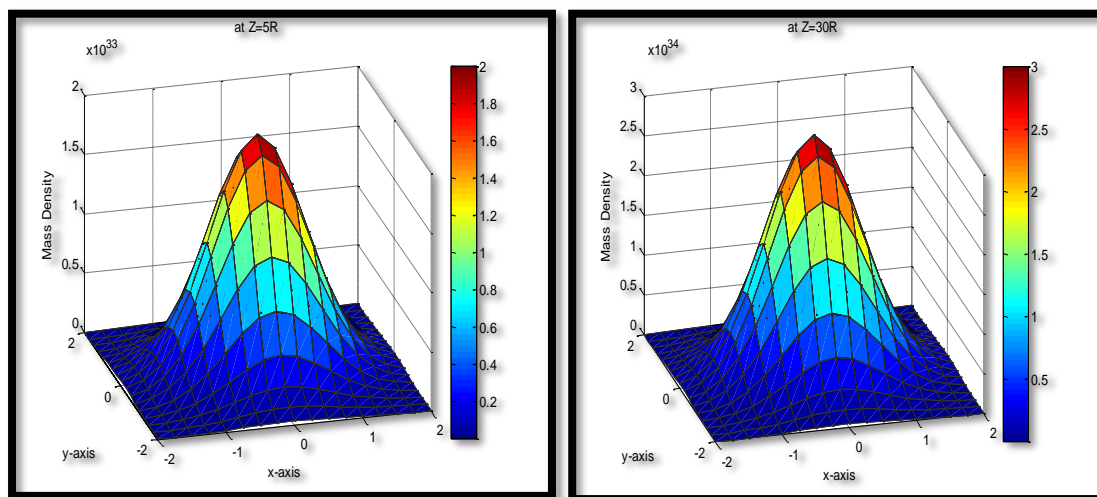
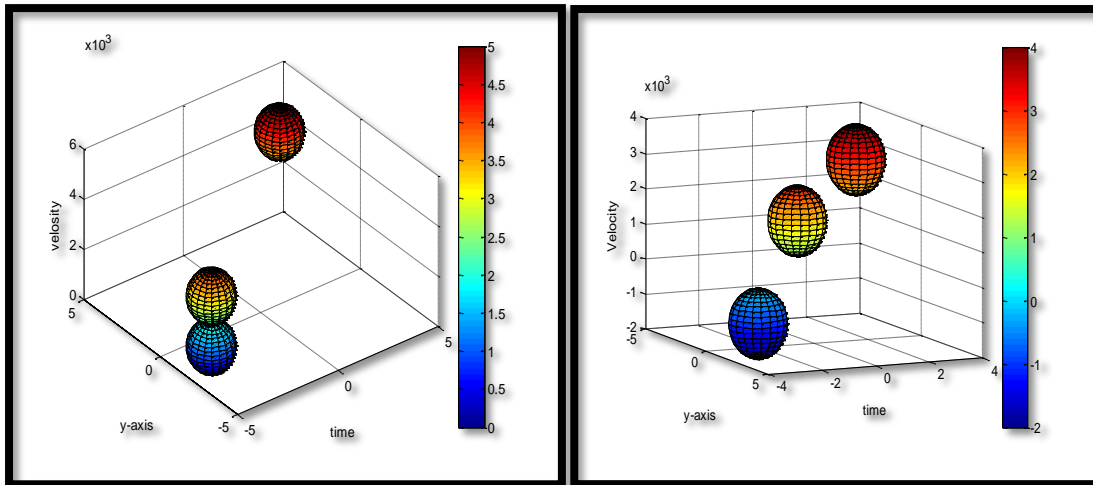


Figure (4): The emerging of CME1 from Sun into interplanetary in term of R_⊙ in two intervals, Z=5 R_⊙ and Z= 30 R_⊙ using the ideal MHD model simulation in three-dimension for a mass density.



Figure(5): Simulation of the velocity for CME1 emerging from Sun into interplanetary using ideal MHD model in three- dimension

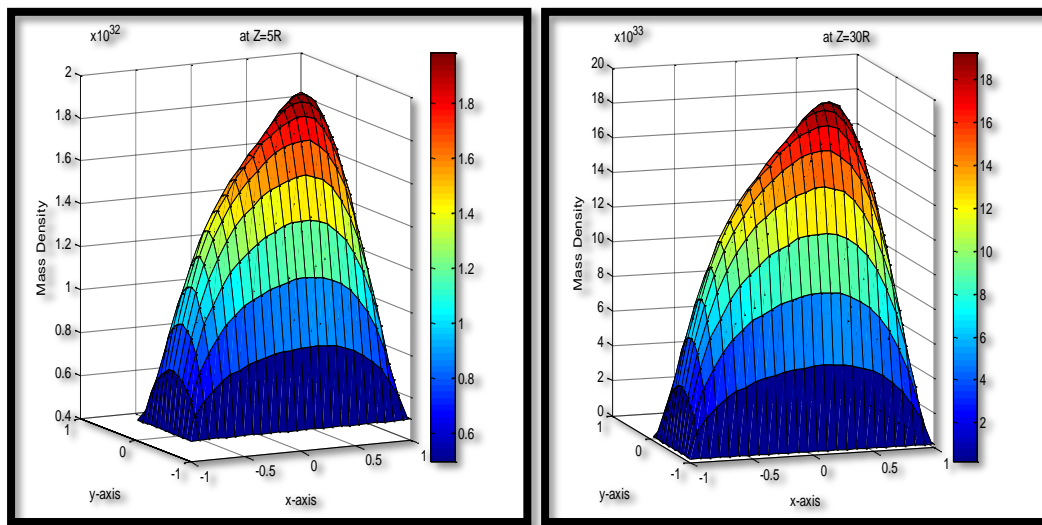
Figure(5) illustrates the simulation in term of the velocity for CME1 at start time 4:12 UT from Sun into interplanetary by using ideal MHD model in three-dimension.

The initial and boundary conditions for the CME2 also was calculated as in table(4), and its numerical simulation was shown in figure (6) by using the equation (1) in term of its mass density, from this figure found that the peak was $\approx 1.8 \times 10^{32}$ at $Z=5R_{\odot}$ and $\approx 17 \times 10^{33}$ at $Z= 30R_{\odot}$. Figure (7) represents the numerical simulation of CME2 by means of its velocity with start time 20:57 UT from Sun into interplanetary using ideal MHD model in three-dimension.

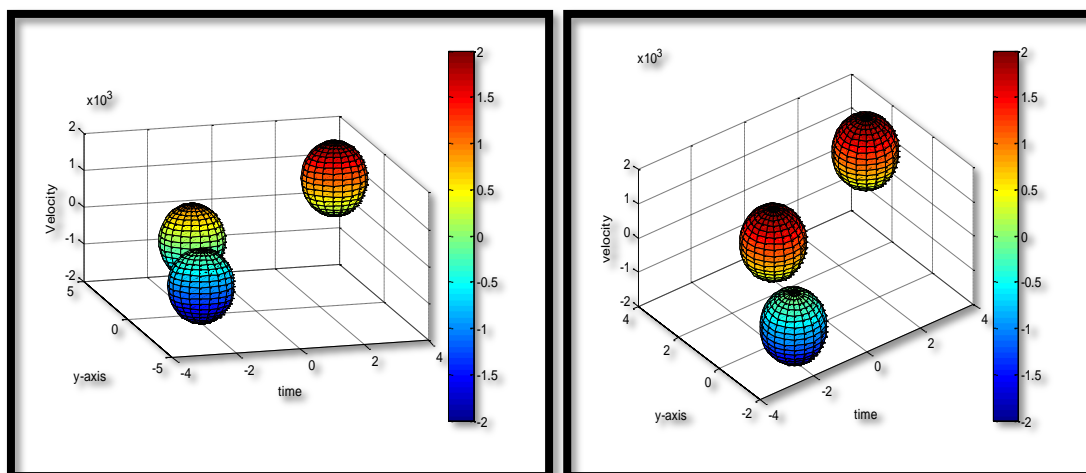
Table (4): Initial and boundary conditions for the CME2

Quantity	Initial value	Boundary value
Mass density, (P)[Kg.m ⁻³]	10^{-14}	0.5
Particle velocity(v_x, v_y, v_z)[Km. S ⁻¹]	1	10^{-3}

Magnetic field, $[B_x, B_y, B_z][nT]$	10^{-6}	5.00
Pressure, (P)[nPa]	10^{-9}	10^{-10}



Figure(6): The simulation of the emerging CME2 from Sun into interplanetary by means of its mass density using ideal MHD model in three-dimensions



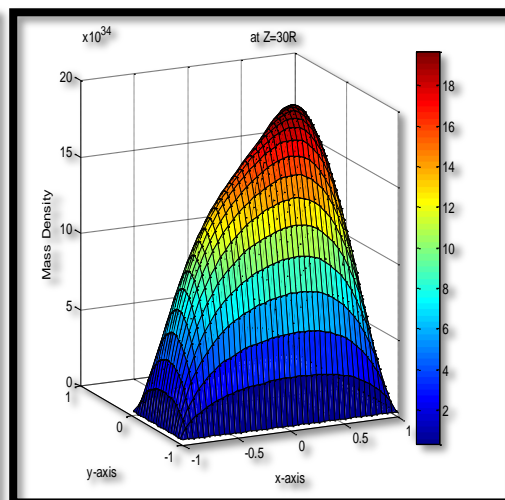
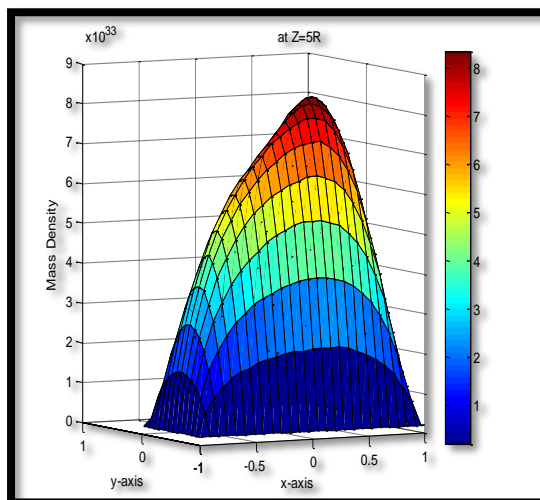


Figure(7). Velocity simulation of the CME2 emerging from Sun into interplanetary using ideal MHD model in three-dimensions

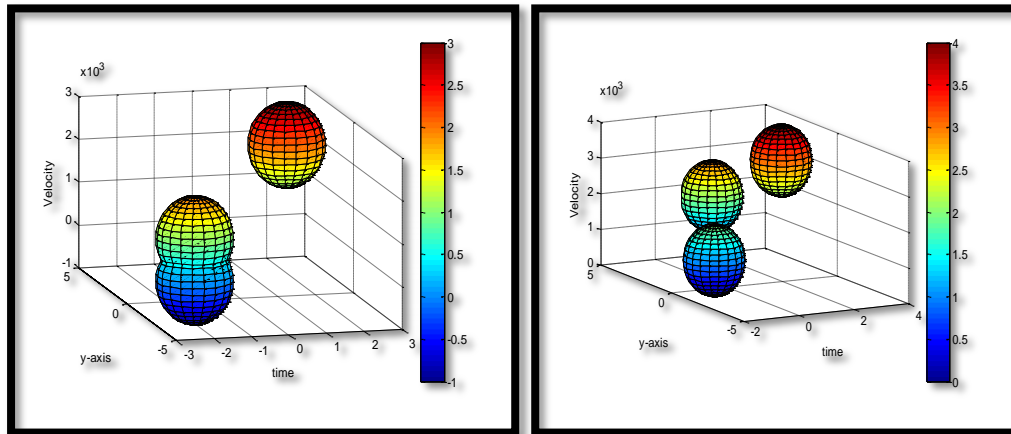
As well as the numerical simulation of CME3 have been clarified in figure (8) in terms of mass density and figure (9) in terms of velocity by using ideal MHD model in three- dimensions. From figure (8) it was found that at $Z= 5R_{\odot}$ the peak $\approx 8 \times 10^{33}$ and at $Z= 30R_{\odot}$ the peak $\approx 16 \times 10^{34}$, and in figure (9) it was found that the start time of CME3 from the sun was at 13:25 UT depending on the initial and boundary conditions illustrated in table(5).

Table(5): Initial and boundary conditions for the CME3

Quantity	Initial value	Boundary value
Mass density, (P)[Kg.m ⁻³]	10^{-15}	0.00
Particle velocity(v_x, v_y, v_z)[Km. S ⁻¹]	10	2×10^{-3}
Magnetic field, [B_x, B_y, B_z][nT]	10^{-6}	2.00
Pressure, (P)[nPa]	10^{-10}	10^{-11}



Figure(8): The simulation of the emerging CME3 from Sun into interplanetary in term of its mass density using ideal MHD model in three-dimension



Figure(9): represents the velocity simulation using ideal MHD model in three-dimension of the emerging CME3 from Sun into interplanetary

All observation of bow shock and the magnetosphere of Jupiter were taken from Voyager 1 in order to use them in the present numerical simulation. The model was based on the combination of these observation and output data from MHD model simulation of the adopted CMEs. Starting from a model of CMEs plasma and the configuration of the magnetic field near Jupiter, at time $t=0$ image dipole was placed upstream of Jupiter to accelerate the formation of its magnetosphere to assure $\nabla \cdot B = 0$ throughout the simulation box. Because Alfven speed becomes very huge near the magnetosphere of Jupiter so the inner boundary of the simulation was placed at $15R_j$ away from Jupiter in order to keep the time step from getting very small. The simulation parameters are fixed at the inner boundary and azimuthally velocity was set, as well as pressure and density of Jupiter were set to determined value from voyager 1. Jupiter equatorial field is about 4.3G and CMEs does not penetrate more than $0.5R_j$ above the surface, this indicated that Jupiter atmosphere is well shielded from washout by magnetic field (0.5-1.0 G). Figure (10), (11), (12) and (13) shows



the interaction

CMEs

and Jupiter

Name	Value
------	-------

between

magnetic field

magnetic field

on the equatorial plane at $t = 00:20, 01:00, 01:20$ and $03:00$ hour. CME approaches the planetary magnetosphere at $t = 00:20$ hour and this CME characterize by a dense hot plasma . In this investigation CME expands through the solar corona and accelerate and pushing the surrounding coronal plasma outward and interacting with the own magnetic field, so the CME deflected and adiabatically expands around the magnetosphere and covers it from sides " at $t = 01:00$ hour" as well as the CME slowed down and then its temperature is drop. At $t = 1:20$ hour, CME reaches the planetary magnetic field which is in the dark side, so at $t = 3:00$ the magnetosphere starts to cover the initial impact and starts to be larger as well as the magneto tail will stretch toward into the interstellar direction because of the ambient plasma. Since the CMEs moves faster than the sound a shock will form a head of it. The speed of the CMEs when it is ejected from the low corona of the Sun will accelerated in the interplanetary and will accede Alfven speed and a fast MHD shock forms with a convex surface which forces outward " Semi-relativistic MHD model". From the data of this investigation, the initial and boundary conditions illustrated in table(6).Table (7) represents the properties of Jupiter [21].

Table (6): Initial and boundary condition used in semi-relativistic MHD application

Quantity	Initial value	Boundary value
Mass density, $(P)[\text{Kg.m}^{-3}]$	0.01	0.09
Particle velocity(v_x, v_y, v_z)[Km. S^{-1}]	1.5	10.00
Magnetic field, $[B_x, B_y, B_z][\text{nT}]$	0.1	0.8
Pressure, $(P)[\text{nPa}]$	0.045	0.360

Table (7): The properties of Jupiter used in this investigation[21][19]



Mass	$1.8986 \times 10^{27} \text{ Kg}$
Radius	71492 Km
Mass density	1.326 g/cm^3
Magnetic field	1 nT
Alfven speed	400 Km/sec
Magnetic moment	$1.5 \times 10^{20} \text{ T. m}^3$
Bow shock distance	$\sim 82 R_j$
Magnetopause distance	50-100 R_j
Magneto tail length	Up to 7000 R_j

Figure (10) shows the north-south components of the magnetic field and flow vectors for Jupiter by taking 20.05 hour and 34.28 hour after the turning of the north ward interplanetary magnetic field (IMF). The simulation of reconnection occurred from $0.78 R_j$ to $1.25 R_j$ down the tail with period between 34hour and 98 hour.

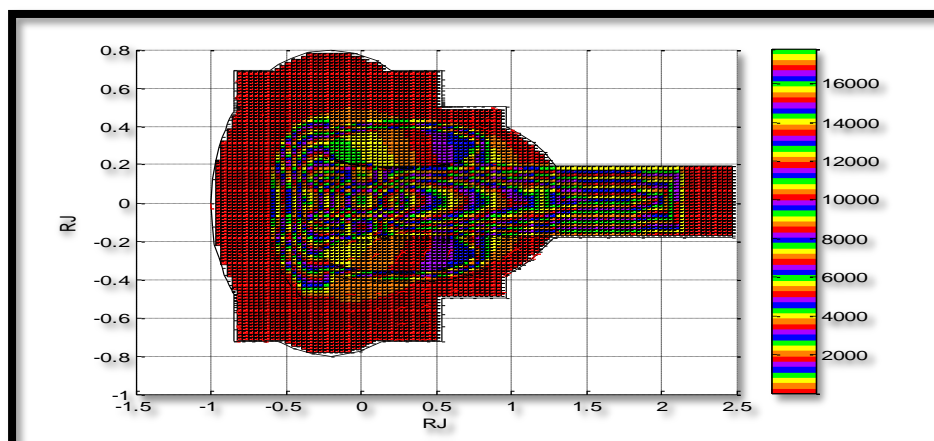
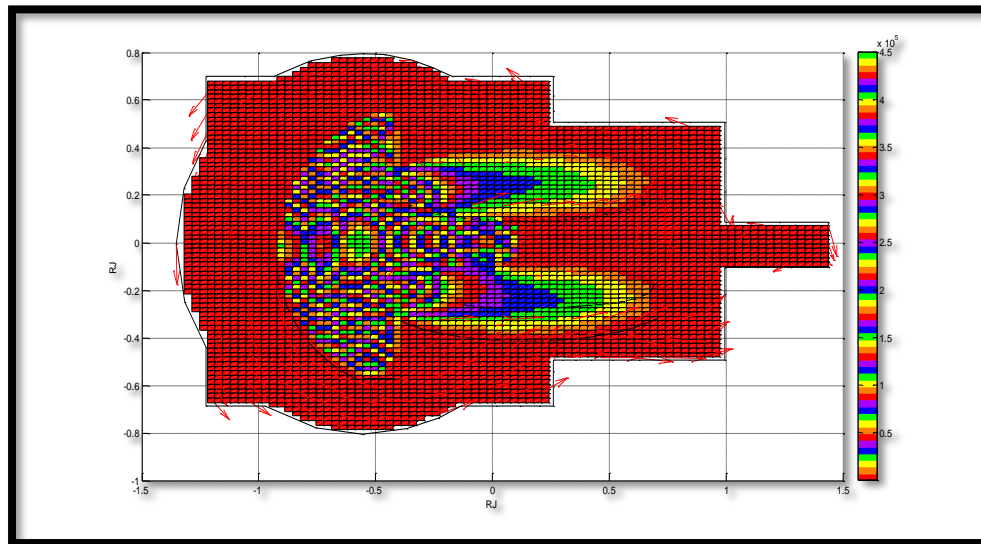
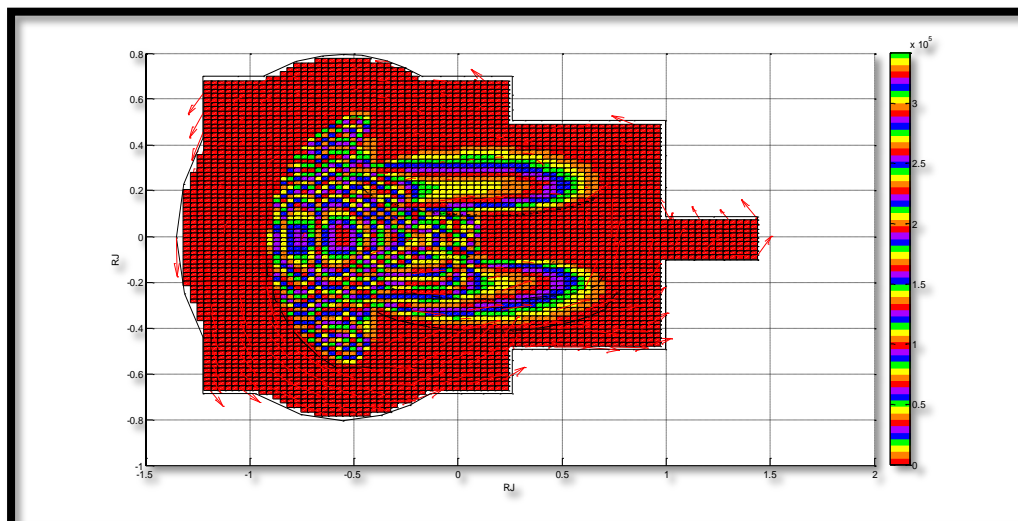


Figure (10): Jupiter magnetic field with B_z component at $0.75 R_j$ equatorial plane by simulation. The colors bars represents magnetic field (nT)

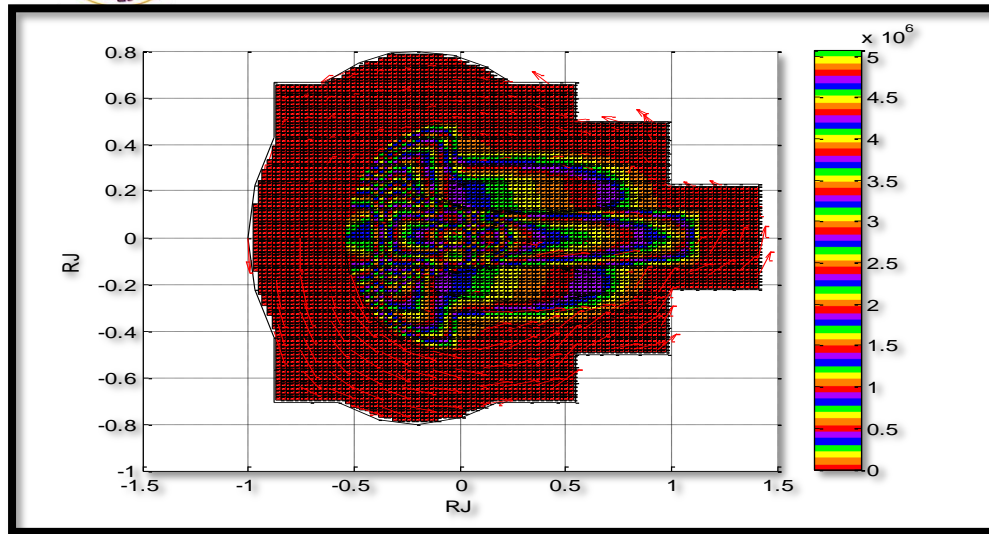
By making use of the equations (8) and (17) figures (11), (12) and (13) represents the interaction between each of the adopted CME1, CME2 and CME3 magnetic field respectively and the Jupiter magnetic field using the semi- relativistic MHD model through the numerical simulation by Leapfrog.



Figure(11): The interaction between the CME1 magnetic field and Jupiter magnetic field (nT) by simulation. The color bars represents the magnetic field in (nT).



Figure(12): The interaction between the CME2 magnetic field and Jupiter magnetic field (nT) by simulation. The color bars represents the magnetic field in (nT).



Figure(13): The interaction between the CME3 magnetic field (nT) and Jupiter magnetic field (nT) by simulation. The color bars represents the magnetic field in (nT)

Another simulation have been held in figures (14), (15) and (16) which represents the interactions between the adopted CMEs and Jupiter in term of the dynamic pressures of them in the noon-midnight meridian plane and down-dusk meridian plane. The interplanetary magnetic field (IMF) was set to zero for these simulations, the used pressures range were from 0.045 nPa to 0.36 nPa and they were selected by scaling the mean dynamic pressure of Jupiter orbit 0.092 nPa by factor of two and because the movements of the bow shock and magnetopause toward Jupiter with increasing pressure, so the sharp pressure at boundary was tabulated. It has been observed that the distance between the bow shock and the magnetopause varied by ratio between 1.31 and 1.24 by inverse relation with the dynamic pressure.

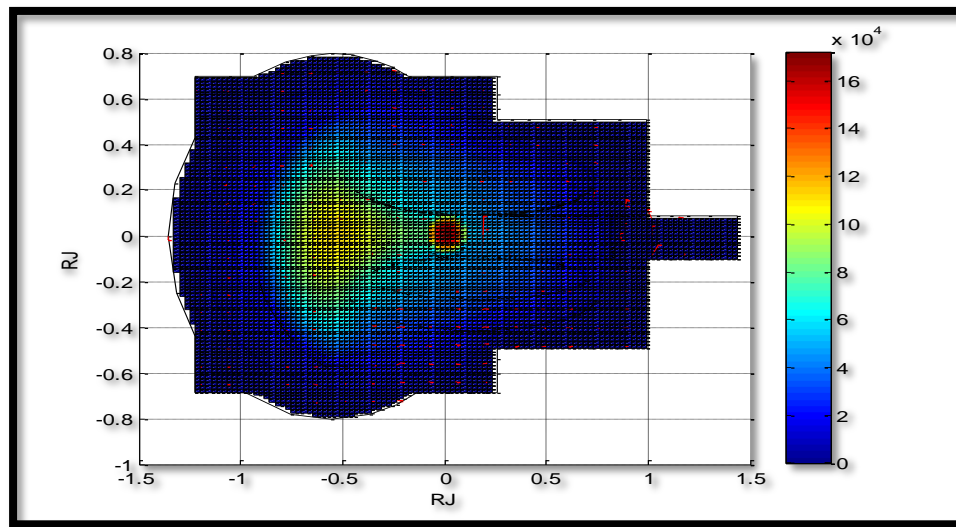


Figure (14): Illustrates the simulation of the pressure contours in the down-dusk meridian plane for the interaction between the CME1 and Jupiter. The color bar gives the values of the dynamic pressures (nPa)

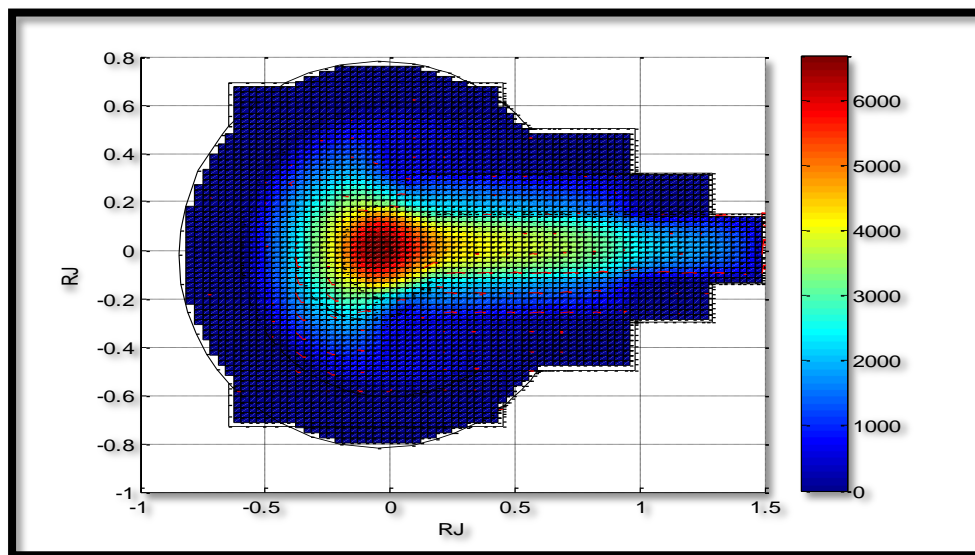


Figure (15): Illustrates the simulation of the pressure contours in the down-dusk meridian plane for the interaction between the CME2 and Jupiter. The color bar gives the values of the dynamic pressures (nPa)

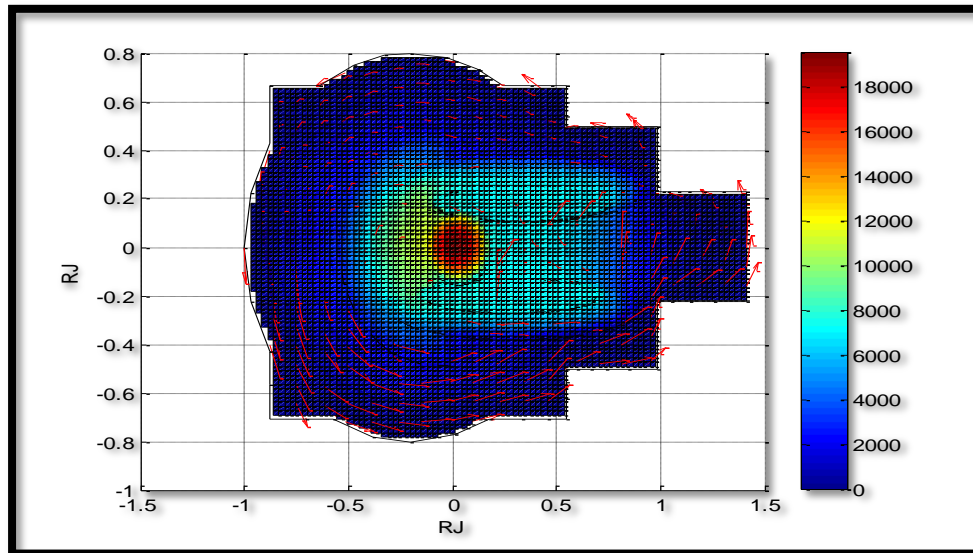


Figure (16): Represents the simulation of the pressure contours in the down-dusk meridian plane for the interaction between the CME3 and Jupiter. The color bar gives the values of the dynamic pressures (nPa)

Note from figure(14) that the plasma sheet is reflected in an irregularly magnetopause in $X=0$ plane. And the asymmetry of the down dusk reverse for small dynamic pressure.

In figure (15) the simulation in term of the dynamic pressure was plotted in XZ-plane " $B_y = 0.42$ nT " and IMF pointing toward the dusk. The CMEs dynamic pressure is 0.09 nPa and the relating fits for $B_{IMF} = 0$. The magnetopause and bow shock are located with solid and dashed lines respectively. Reconnection take place near the equator on the side of the magnetopause when IMF pointing in the Y-direction and the addition of IMF to B_y does not change the standoff distance at the bow shock and magnetopause.

Figure (16) represents the simulation of the dynamic pressure plotted in YZ- plane and the IMF was in Y-direction ($B_y = 0.105$ nT) and pointing toward the dusk as well as the dynamic pressure of the CME here is 0.09 nT for the fitting of $B_{IMF} \neq 0$, the



bow shock and the magnetopause location were shown with solid and dashed lines respectively. And the magnetopause rotates around Sun-Jupiter line of $B_y \neq 0$.

8. CONCLUSIONS

Studying the interaction of the magnetic field of Jupiter with the magnetic field of the CME using numerical simulation is of great importance, first, because Jupiter is a giant planet in the solar system and its orbital synchronizes with the orbital of Earth so it is responsible for preventing approaching comets and meteorites invading the inner Solar System, and thereby protecting the Earth from bombardment. Second, the interplanetary region controlled by Jupiter's magnetic field (i.e. the magnetosphere) and solar wind, there is a power struggle between the solar wind and Jupiter's magnetosphere and this interaction should be understood and what effect on the interplanetary, this interaction is important for the countless magnetic objects across the galaxy. When Sun ejects streams of particles into space as giant storm erupt, the solar wind become much stronger and compress Jupiter's magnetosphere and will lead to an extension of the magnetosphere of Jupiter to cover most of the planets of synchronized orbit with Jupiter and the most notably is the Earth.

Generally, it could be said that this study is important for the development of space technology. The analysis of this investigation covered the interaction between Jupiter's magnetic field and coronal mass ejections (CMEs) magnetic field for the rising phase of Solar cycle 24 for the years 2011, 2012 and 2013.

From this study It was found that the CMEs for the adopted events which reaches Jupiter are of the impulsive types and are often associated with solar flares. The CMEs moved uniformly across the interplanetary at speeds higher than 800 Km s^{-1} , where the speed of CME1= 1610 Km s^{-1} , the speed of CME2 = 1966 Km s^{-1} and the CME3 = 861 Km s^{-1} , so they push the slower CMEs a side by moving against its spreading ambience and compress it, then the interplanetary magnetic field will compress also and drops around the CMEs. Since the mass moves faster than the sound, a bow shock will formed a head of it, because in the low corona sound speeds is about 150 Km s^{-1} and Alfven speed is $500\text{-}1000 \text{ Km s}^{-1}$, both speeds decrease in



going out the Sun. So, when CME travels in speed more than Alfven speed, a fast MHD shock form with convex surface which faces out ward and this can be seen in figures (11), (12) and (13), and also from these figures it was noted that the interaction between the magnetic fields of CMEs and Jupiter increase as the speed of CMEs increased.

As well as it has been concluded that the MHD model which was used in the simulation of this study is an advanced model and enhances the present analysis, where by using the ideal model (conservative), the algorithm could be develop to a new state to create another model which is non- conservative model which was used in this study, which is called the Semi- relativistic MHD model.

Also it was concluded from this approach, the Leapfrog method has a higher order of accuracy and it is convenient for this study more than other approximations and be stable when the time iteration $dt < 0.1$ and the increasing of mesh size will increase the runtime totally, so a suitable choosing of mesh was give a good numerical results.

REFERENCES

- [1] Vourlidas, A., Howards, R., 2006, APJ, Vol 642, p.1216.
- [2] Zaki, W., Abdullah, M., 2014, " Studying the space weather of rising phase for solar cycle 24 through its activity", Salahaddin University, MsC thesis.
- [3] Sharma, A., Verma, S., 2013, " Solar cycle during the rising phase of solar cycle 24", IJAA, Vol. 3, No. 3.
- [4] Forbes, T., Linker, J., Chen, J., Cid, C., Kota, J., Lee et al, 2006, " CME theory and models" space science reviews, Vol.123, 251-302.
- [5] Barbu, V. et al., 2003, " Exact controllability magneto-hydrodynamic equations". Communications on pure and applied mathematics. Vol. 56, Issue 6,732-783.
- [6] Encrenaz, T., Birbing, T., and Blanc, M., 2003, " The solar system", Berlin, DE: Springer, ISBN 3540002413.



- [7] Delamere, P.A., and Bagenal, F., 2010, "Solar wind interaction with Jupiter's magnetosphere", Journal of Geophysics Research. Vol. 115, Issue A10, A10201.
- [8] Lugaz, N., Manchester IV, W.B. and Gombosi, T.I., 2005, " The evolution of coronal mass ejection density structures", Center for space environment Modeling, University of Michigan, The Astrophysical Journal, Vol. 627, Issue 2, pp.1019-1030
- [9] Rauer, H., et al, " 3D- MHD simulation of the effect commoving discontinuities in the solar wind on cometary plasma tails", Astronomy and Astrophysics, Vol.295, No. 2, p. 529-550, 1995.
- [10] Toth, G., Van der holst, B. et al, 2012, " Adaptive numerical algorithms in space weather modeling", Journal of Computational Physics, Vol. 231, Issue 3, P. 870-903
- [11] Meng, X., Tóth, G., Sokolov, I.V., Gombosi, T.I., 2012, "Classical and Semi relativistic Magneto hydrodynamics with Anisotropic Ion Pressure ", Journal of Computational Physics, Vol. 231, p. 3610-3622.
- [12] Boris, J. P., 1970, "A physically Motivated Solution of the Alfven Problem ", Tech. Report NRL Memorandum Report 2167 (Naval Research Laboratory, Washington, DC
- [13] http://www.srl.utu.fi/ERNE_data
- [14] Allawi, H., 2010, " Evaluation of the methods of calculating the first acceleration of solar energetic particles in solar corona according to ERNE/ SOHO measurements", Ph.D. thesis, College of Science, University of Basra, Iraq.
- [15] Al-swad, A., 2009, " Multi-Eruption solar energetic particles events observed by SOHO/ ERNE", Ph.D. thesis, University of Turku, Finland.
- [16] Zaidan, A. S., 2016, " Studying and analysis the intensity –time profile of the energetic protons associated with solar eruption", Ph.D thesis, University of Kirkuk, Iraq.



- [17] Zaki, W., Zidane, A., Al-sawad, A., 2016, " Photometric and statistical analysis of solar energetic particle (SEP) for the peak of solar cycle 24", International Journal of Astronomy and Astrophysics, Vol. 6, No. 3, p. 276-287
- [18] http://cdaw.gsfc.nasa.gov/CME_list/
- [19] Williams, D. R., "Jupiter Fact Sheet ", NASA. Retrieved August 8, 2007. (November 16, 2004).
- [20] Bagenal, F., and P.A. Delamere, 2011, "Flow of mass and energy in the magnetospheres of Jupiter and Saturn ", J. Geophys. Res., 116, A05209.
- [21] Bolton, S. J. the Juno Science Team., 2010, "The Juno mission in Proceedings IAU Symposium No. 269", eds C. Barbieri, S. Chakrabarti, M. Coradini, and M. Lazzarin (Padova: International Astronomical Union).